JOURNAL OF SOLID STATE CHEMISTRY **122,** 7–14 (1996)
ARTICLE NO. 0073

TTB Structure of $K_4Ce_2M_{10}O_{30}$ (M = Nb or Ta): Crystal Growth and Joint X-Ray and HREM Studies

Fouad Brik, Renée Enjalbert, Christian Roucau, and Jean Galy

Centre d'Elaboration de Matériaux et d'Etudes Structurales, C.N.R.S., 29 rue Jeanne Marvig, B.P. 4347, 31055 Toulouse Cedex, France

Received July 17 1995; accepted October 19, 1995

$K_4Ce_2Nb_{10}O_{30}$ and $K_4Ce_2Ta_{10}O_{30}$ phases have been synthesized respectively at 1200 and 1250°C. Single crystals grown at high temperature, respectively, 1400 and 1650°C, and X-ray studies have shown that these isostructural phases crystallize in the tetragonal system with the tetragonal tungsten bronze structure (TTB). The lattice constants are $a = 12.537(1)$ and $c = 3.8976(7)$ Å for Nb phase and $a = 12.515(2)$ and $c = 3.888(1)$ Å for Ta phase. Magnetic measurements indicate cerium in the +III oxidation state. Both crystal structures of Nb and Ta phases have been determined and refined to reliability factors down to $R_{Nb} = 0.048$ (785 *hkl*) and $R_{Ta} = 0.032$ (836 *hkl*). In these highly stoichiometric TTB structures, the K atoms fill the pentagonal tunnels with a tricapped trigonal prism of coordination polyhedra of oxygens, and the Ce atoms, filling the tetragonal tunnels, are in almost perfect cubooctahedra (CN = 12). An investigation by electron microscopy at high resolution (HREM) establishes the remarkable regularity of the lattice, making it possible to precisely localize the various metals Nb, Ce, and K.

INTRODUCTION

As early as 1838 potassium tungsten bronzes were reported (1). A hundred years later A. Magnéli determined both tetragonal (TTB) and hexagonal (HTB) structures of these remarkable K_xWO_3 phases (2, 3). Since that time they have been the center of considerable interest, many nonstoichiometric A_xMO_3 phases, with the TTB structure, being synthesized with A = alkali, alkaline earth, rare earth

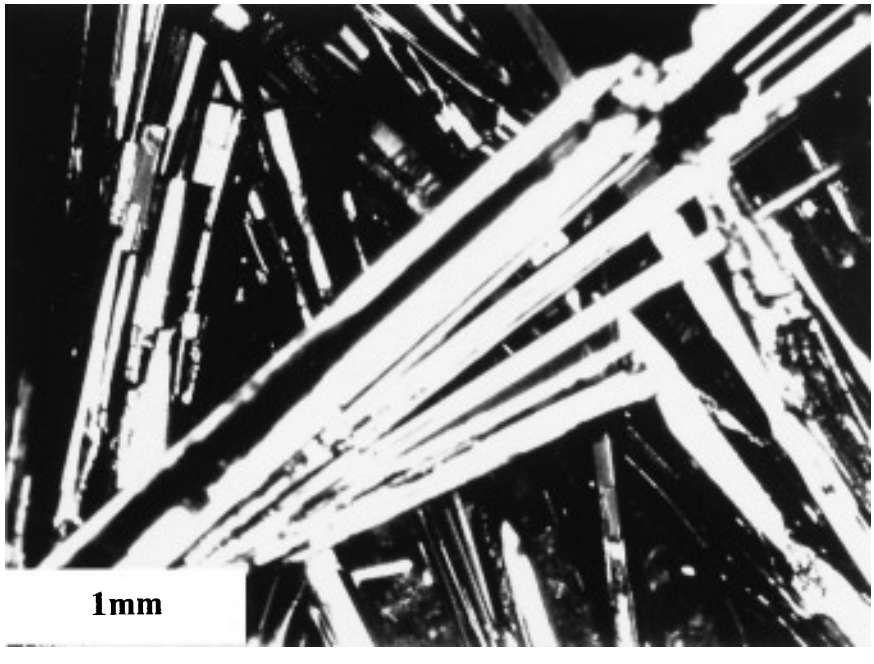

FIG. 1. Morphology of the crystals of $K_4Ce_2Nb_{10}O_{30}$ elongated along the **c** axis.

0022-4596/96 $18.00

TABLE 1
Analytic Results for $K_4Ce_2M_{10}O_{30}$ (M = Nb or Ta)

	Molar concentration (%)				
Atom	K	Ce	Nb	Ta	O[a]
Calculated	8.69	4.35	21.74	0	65.22
	8.69	*4.35*	*0*	*21.74*	*65.22*
Experimental	8.7	4.5	21.7	0	65.1
Chemical analysis	*9.1*	*4.5*	*0*	*21.7*	*64.7*
Experimental	7.6	4.5	21.8	0	66.1
Microprobe	*7.5*	*4.6*	*0*	*22.1*	*65.8*

[a] Calculated by difference.

... and M = transition elements like Ti, V, Mo, W, Nb, and Ta (4–11 for example). Structure relationships have also been established between TTB and HTB structures (12) as well as with ReO_3 (13). Our recent investigations on oxide systems based on niobates allowed us to stabilized the scheelite form of $LaNbO_4$ at room temperature by substituting some vanadium atoms into niobium, i.e., $LaNb_{0.7}V_{0.3}O_4$ (14). When these researches were extended to niobates containing simultaneously an alkali (potassium) and a rare earth (cerium), a stoichiometric phase with the TTB structure was obtained, $K_4Ce_2Nb_{10}O_{30}$. We report in this paper this synthesis, crystal growth, characterization, single-crystal X-ray, high resolution electron microscopy (HREM) studies of this phase together with its tantalum homologue.

TABLE 2
Physical and Crystallographic Data and Parameters for Data Collection and Refinement for $K_4Ce_2M_{10}O_{30}$ (M = Nb or Ta)

	Crystal data	
Formula	$K_{0.4}Ce_{0.2}NbO_3$	$K_{0.4}Ce_{0.2}TaO_3$
Crystal system	Tetragonal	Tetragonal
Space group	$P4/mbm$(n°127)	$P4/mbm$(n°127)
a [Å]	12.537(1)	12.515(2)
c [Å]	3.8976(7)	3.888(1)
V [Å]	612.6(1)	608.9(2)
Z	10	10
Molecular weight	184.57	272.61
ρ calc [g/cm^3]	5.00	7.43
μ [Mo$K\alpha$ cm^{-1}]	88	516
Morphology	Parallepiped	Parallepiped
Color	Brown	Yellow
Dimension (mm)	0.05 × 0.075 × 0.125	0.025 × 0.038 × 0.125
	Data collection	
Temperature [°C]	20	20
Wavelength [Mo$K\alpha$][Å]	0.71069	0.71069
Monochromator	graphite	graphite
Scan mode	ω-2θ	ω-2θ
Scan width [°]	0.90 + 0.35 tan θ	0.80 + 0.35 tan θ
Take-off angle [°]	4.5	4.0
Max Bragg angle [°]	35	40
T_{max}[s]	60	80
	Control reflections	
Intensity (every 3600 s)	−6 −2 0/−12 0 0/0 12 0	−6 2 0/−8 −2 0/6 2 −2
Orientation (every 150 refl.)	−4 −1 −1/1 −1 −3	2 −1 −3/4 5 −2
	Structure refinement	
Reflections for cell refinement	25 with 6 ≤ θ ≤ 20°	25 with 6 ≤ θ ≤ 20°
Reflections collected	2902	1585
Reflections unique measured	785	888
Reflections unique used	785	836 ($I > 3\ \sigma(I)$)
Parameters refined	41	41
Weighting	$w = 1$	$w = 1$
$R = \Sigma \|\|F_o\| - \|F_c\|\|/\Sigma\ \|F_o\|$	0.048	0.032
$R_w = [\Sigma w(\|F_o\| - \|F_c\|)^2/\Sigma wF_o^2]^{1/2}$	0.059	0.036

TABLE 3
Final Least-Squares Atomic Parameters for $K_4Ce_2M_{10}O_{30}$ (M = Nb or Ta)

Atom	Site	Occ.	x	y	z	B_{eq} (Å^2)
Nb1	2c	1	0	1/2	1/2	1.89(7)
Nb2	8j	1	0.07523(7)	0.21514(7)	1/2	0.47(3)
Ce	2a	1	0	0	0	0.54(2)
K	4g	1	0.1715(2)	0.6715(2)	0	2.0(1)
O1	2d	1	0	1/2	0	2.7(7)
O2	8i	1	0.076(1)	0.1941(8)	0	2.2(4)
O3	8i	1	−0.0028(7)	0.3431(7)	1/2	1.3(3)
O4	8j	1	0.1313(8)	0.0620(7)	1/2	1.5(3)
O5	4h	1	0.2853(7)	0.7853(7)	1/2	0.8(2)

Atom	U_{11}	U_{22}	U_{33}	U_{12}
Nb1	0.0090(5)	0.0090(5)	0.053(2)	0.0013(7)
Nb2	0.0078(3)	0.0047(3)	0.0050(3)	−0.0008(3)
Ce	0.0065(3)	0.0065(3)	0.0071(4)	0
K	0.028(1)	0.028(1)	0.016(2)	−0.016(2)
O1	0.043(8)	0.043(8)	0.013(8)	−0.01(1)
O2	0.054(7)	0.020(4)	0.008(3)	−0.014(4)
O3	0.014(3)	0.010(3)	0.026(4)	0.002(3)
O4	0.025(4)	0.015(4)	0.016(3)	0.009(3)
O5	0.011(3)	0.011(3)	0.009(4)	0.003(3)

Atom	Site	Occ.	x	y	z	B_{eq} (Å^2)
Ta1	2c	1	0	1/2	1/2	0.55(2)
Ta2	8j	1	0.07642(3)	0.21440(3)	1/2	0.25(1)
Ce	2a	1	0	0	0	0.46(2)
K	4g	1	0.1691(3)	0.6691(3)	0	2.5(2)
O1	2d	1	0	1/2	0	2.8(4)
O2	8i	1	0.075(1)	0.1929(9)	0	2.1(3)
O3	8j	1	−0.001(1)	0.3430(8)	1/2	1.8(3)
O4	8j	1	0.1312(8)	0.0621(7)	1/2	1.2(3)
O5	4h	1	0.2832(7)	0.7832(7)	1/2	0.9(2)

Atom	U_{11}	U_{22}	U_{33}	U_{12}
Ta1	0.0048(2)	0.0048(2)	0.0109(4)	0.0011(2)
Ta2	0.0042(1)	0.0029(1)	0.0023(1)	−0.0004(1)
Ce	0.0056(2)	0.0056(2)	0.0060(4)	0
K	0.040(2)	0.040(2)	0.015(2)	−0.028(2)
O1	0.038(5)	0.038(5)	0.030(5)	0.027(5)
O2	0.052(5)	0.018(4)	0.007(3)	−0.018(4)
O3	0.017(3)	0.007(3)	0.043(4)	0.006(3)
O4	0.016(3)	0.004(3)	0.026(3)	0.000(3)
O5	0.005(2)	0.005(2)	0.024(4)	0.005(3)

Note. $B_{eq} = 8\pi^2/3$ trace u (u diagonalized U matrix); $U_{13} = U_{23} = 0$.

EXPERIMENTAL

Synthesis

The $K_4Ce_2M_{10}O_{30}$ (M = Nb and Ta) phases were prepared by reacting K_2CO_3, CeO_2, and M_2O_5 in the 2:2:5 proportions. The mixtures finely grounded were heated at about 750°C for up to 5 hrs; the products were then regrounded, heated again, the temperature being raised at a rate of 100°C/min up to 1200°C (or 1250° for Ta), and maintained at this temperature for 24 hrs. The samples, controlled by optic microscopy and X-ray powder patterns, were obtained as homogeneous powders, pale brown for niobium and yellow for tantalum compositions. The reaction equation implies losses of CO_2 and O_2 by thermal decomposition of K_2CO_3 and CeO_2:

$$2\,K_2CO_3 + 2\,CeO_2 + 5\,M_2O_5 \rightarrow K_4Ce_2M_{10}O_{30} + 2\,CO_2\uparrow + \tfrac{1}{2}\,O_2\uparrow.$$

The protocol to grow single crystals of these phases was as follow: heating from 750 up to 1200°C at a rate of 2°C/min and stabilization for 2 hrs at such temperature; and heating from 1200 up to 1400°C at a speed of 4°/min and slow cooling (1°/min) down to 850°C and then to room temperature on the furnace inertia. For Ta samples the protocol increased the temperature to 1270°C for 1200°C and 1650°C for 1400°C.

Characterization

The morphology of the crystals as revealed in Fig. 1 shows a plate-like aspect elongated in the direction of **c** axis. The quantitative analysis on the crystals were performed using a microprobe SX 50 Cameca. On the other hand, energy dispersive spectroscopy was used on a representative selection of single crystals to confirm the presence of K, Ce, and Nb (or Ta). These investigations were conducted on a CM20 Philips electronic microscope fitted with a Tracor system. Chemical as well as microprobe analysis confirmed the composition of the two phases (Table 1). The magnetic susceptibility was measured on a Faraday Balance (Oxford Instrument) at room temperature. The found experimental effective moment for Ce, 2.35 BM, is in excellent agreement with the +III oxydation state of this atom (μ_{eff} = 2.28–2.46 BM (15)).

X-Ray Study

The samples were analyzed by X-ray powder pattern techniques using a XRD 3000 Siefert diffractometer with Cu$K\alpha$ radiation. Single crystals cut again to reasonable size, in order to avoid too drastic an absorption correction, were examined by Laue and precession methods with Mo$K\alpha$ radiation. $K_4Ce_2M_{10}O_{30}$ (M = Nb, Ta) phases crystallize in the tetragonal system. The systematic absences are $k = 2n + 1$ in $0kl$ compatible to the possible space groups $P4/mbm$ (n°127), $P4bm$ (n°100), or $P\bar{4}b2$ (n°117).

The complete data collections were performed using a

TABLE 4
Selected Distances (Å) and Angles (°) for $K_4Ce_2M_{10}O_{30}$(M = Nb or Ta)

Nb1 and Nb2 (or *Ta1* and *Ta2*) environments

Nb1(*Ta1*)	O1	O1i	O3	O3ii	O3iii	O3iv
O1	1.9488(3)	3.8976(7)	2.769(6)	2.769(6)	2.769(6)	2.769(6)
	1.9438(5)	*3.888(1)*	*2.764(7)*	*2.764(7)*	*2.764(7)*	*2.764(7)*
O1i	180	1.9488(3)	2.769(6)	2.769(6)	2.769(6)	2.769(6)
	180	*1.9438(5)*	*2.764(7)*	*2.764(7)*	*2.764(7)*	*2.764(7)*
O3	90	90	1.968(8)	3.935(8)	2.733(9)	2.733(9)
	90	*90*	*1.965(9)*	*3.930(9)*	*2.80(1)*	*2.80(1)*
O3ii	90	90	180	1.968(8)	2.733(9)	2.831(9)
	90	*90*	*180*	*1.965(9)*	*2.80(1)*	*2.80(1)*
O3iii	90	90	92.0(5)	88.0(5)	1.968(8)	3.935(8)
	90	*90*	*90.8(4)*	*89.2(4)*	*1.965(9)*	*3.930(9)*
O3iv	90	90	88.0(5)	92.0(5)	180	1.968(8)
	90	*90*	*89.1(4)*	*90.9(4)*	*180*	*1.965(9)*

Nb2(*Ta2*)	O2	O2i	O3	O4	O4v	O5vi
O2	1.967(1)	3.8976(7)	2.872(9)	2.651(9)	2.719(9)	2.855(9)
	1.962(2)	*3.888(1)*	*2.868(9)*	*2.636(9)*	*2.708(9)*	*2.861(9)*
O2i	164.6(5)	1.967(1)	2.872(9)	2.651(9)	2.719(9)	2.855(9)
	164.2(7)	*1.962(2)*	*2.868(7)*	*2.636(8)*	*2.708(8)*	*2.861(8)*
O3	96.6(3)	96.6(3)	1.878(9)	3.904(9)	2.758(9)	2.821(8)
	96.6(4)	*96.6(4)*	*1.8880(9)*	*3.887(9)*	*2.758(9)*	*2.829(9)*
O4	82.7(3)	82.7(3)	168.7(4)	2.043(9)	2.574(9)	2.988(9)
	82.7(4)	*82.7(4)*	*168.7(5)*	*2.026(9)*	*2.569(9)*	*2.968(9)*
O4v	86.1(4)	86.1(4)	90.1(4)	78.7(5)	2.018(9)	3.971(9)
	85.6(4)	*85.6(4)*	*89.9(4)*	*78.9(3)*	*2.022(9)*	*3.974(8)*
O5vi	93.4(4)	93.4(4)	94.7(4)	96.6(4)	175.3(5)	1.957(8)
	93.8(4)	*93.8(4)*	*95.0(4)*	*96.3(3)*	*175.1(4)*	*1.956(9)*

Ce and K environments

Ce–O2	2.611(9)	×4	*2.592(5)*	×4
Ce–O4	2.667(9)	×8	*2.661(7)*	×8
O–Ce–O range	57.7–62		*57.7–62*	
	86.1–93.9		*86.1–93.9*	
	118–122.3		*117.9–122.3*	
	180		*180*	
K–O3	2.882(7)	×4	*2.866(3)*	×4
K–O5	2.805(6)	×2	*2.805(7)*	×2
K–O1	3.041(7)		*2.992(3)*	
K–O2	3.182(7)	×2	*3.211(4)*	×2
K–O4	3.435(8)	×4	*3.438(3)*	×4

Symmetry code:
i: $x, y, z + 1$, ii: $-x, -y + 1, z$, iii: $-y + \frac{1}{2}, -x + \frac{1}{2}, z$,
iv: $y - \frac{1}{2}, x + \frac{1}{2}, z$, v: $-y, x, z$, vi: $-y + 1, x, z$
vii: $-x, -y, z$, viii: $y, -x, z$, ix: $-x, -y + 1, -z$
x: $-y + \frac{1}{2}, x + \frac{1}{2}, -z$, xi: $-x + \frac{1}{2}, y + \frac{1}{2}, -z$, xii: $-x + \frac{1}{2}, y + \frac{1}{2}, -z$
xiii: $y, -x + 1, z$, xiv: $y, -x + 1, -z$, ′: by center

Note. For clarity, some codes are omitted in this table, but appear in Figs. 3 and 4.

Nonius CAD-4 diffractometer. Preliminary setting angles of 25 *hkl* reflections regularly distributed in the half sphere were automatically optimized and used in least-squares calculation to refined the cell constants. The intensity of the *hkl* reflections have been corrected for Lorentz and polarization factors; absorption correction have been carried out by using an empirical method (16). The values of the atomic scattering factors with their anomalous dispersion were from the usual sources (17). The calculations and some drawings were performed on the vectorial minisupercomputer Alliant VFX80 using SHELX (18) and ORTEP (19) softwares, other drawings being realized on a Macintosh quadra 800.

From the parameters and space groups of these phases it was clear that they were isostructural with Magneli's K_xWO_3 TTB structure. The choice between the three

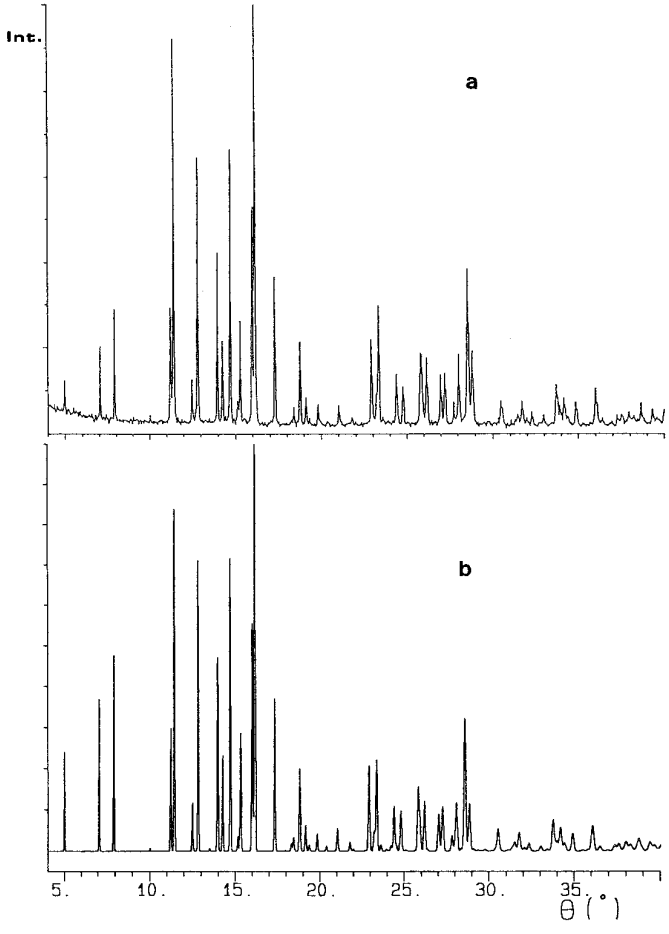

FIG. 2. Experimental (a) and calculated (b) powder patterns of $K_4Ce_2Ta_{10}O_{30}$.

possible space groups was driven to *P*4/*mbm*, taking into account the clear indication of the statistical test which is in favor of a centrosymetric cell. Using the data, the structure determination was then immediately tackled by Fourier methods and full matrix least-squares refinement. Table 2 gives pertinent details concerning the data collection. The final positional and thermal parameters (B's or U_{ij}) of all the atoms appear in Table 3. Interatomic distances and angles are summarized in Table 4. The good fit between experimental and calculated powder patterns is demonstrated for the Ta compound, for example, in Fig. 2.

HREM Study

HREM observations were performed on a Philips CM30 fitted with supertwin pole pieces having a 1.9 Å point resolution. Experimental micrographs were compared to simulated ones computed with NCEMSS software (TEMPAS) (20). HREM experiments were carried out on single crystals. In order to obtain oriented thin films with faces parallel to the (001) planes, the samples were immersed in resin (glue) in such a way that all of the single crystals presented their **c** axis parallel. The samples were then cut perpendicular to this direction. The samples were first mechanically polished, the final thinning to the electron transparency being achieved by ion milling.

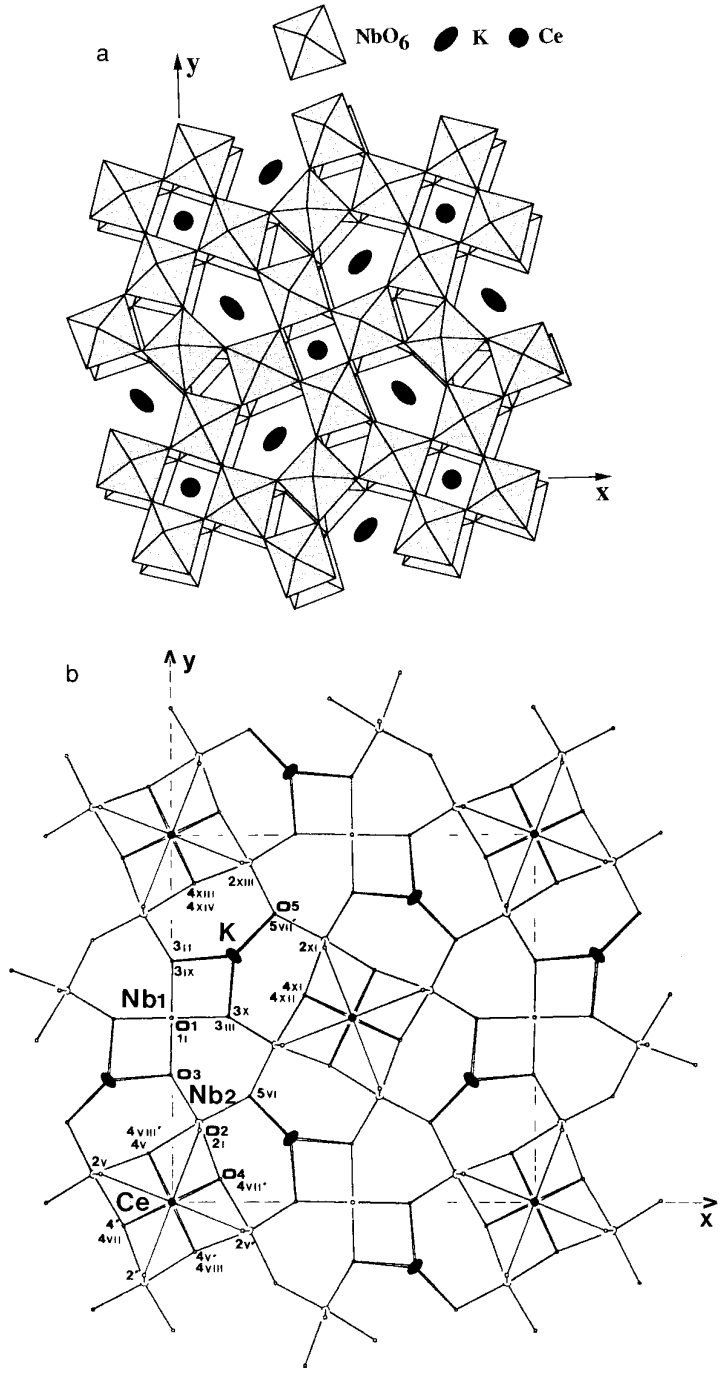

FIG. 3. Structure of TTB phase $K_4Ce_2Nb_{10}O_{30}$: perspective view (a) and projection onto the (001) plane (b).

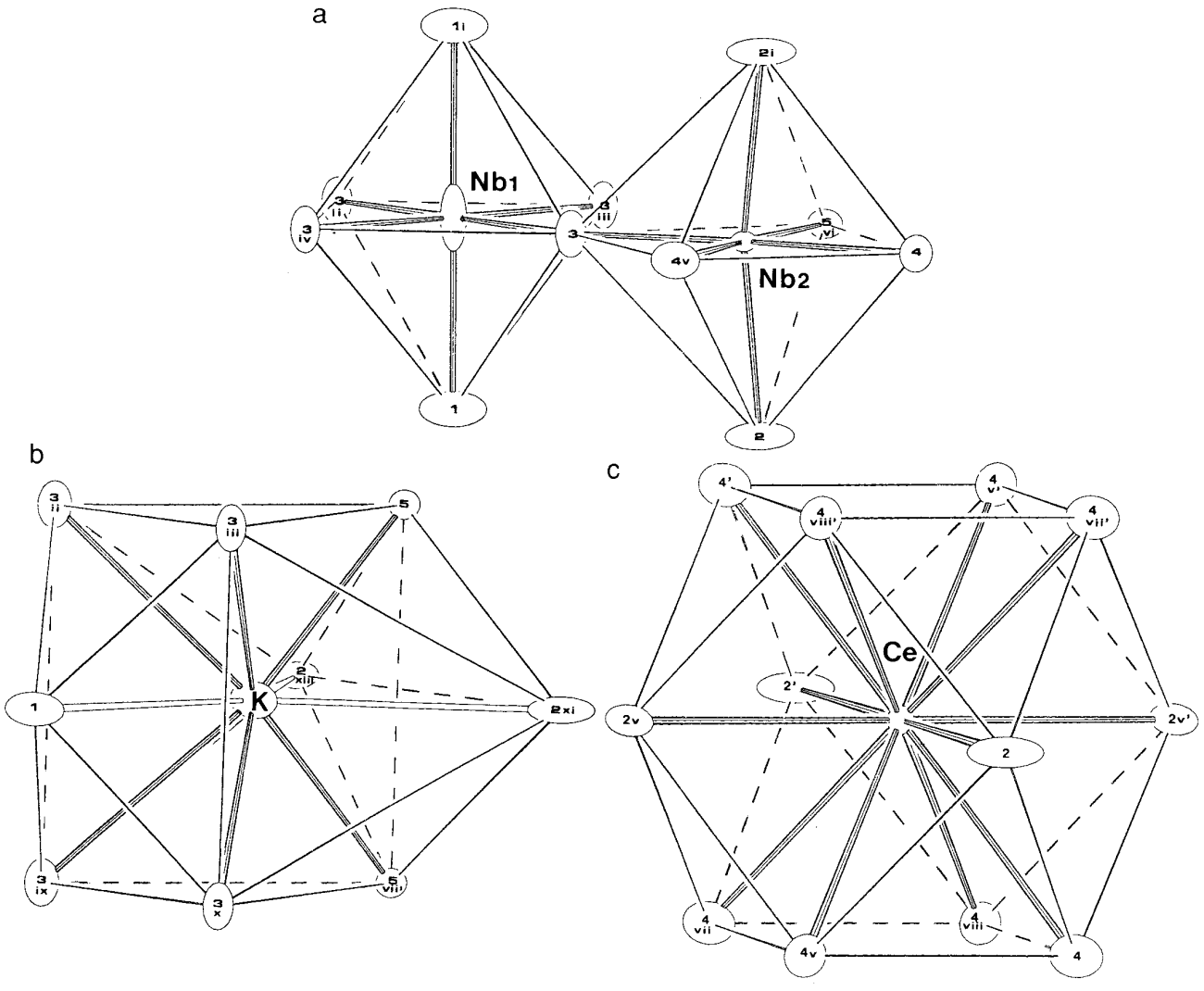

FIG. 4. Environments of niobium (a), potassium (b), and cerium (c) atoms in the $K_4Ce_2Nb_{10}O_{30}$ structure.

DISCUSSION

The perspective view of $K_4Ce_2Nb_{10}O_{30}$ structure along [001] is given in Fig. 3a. The bonding scheme is revealed on the projection of the structure onto the plane (001) in Fig. 3b. This phase can be formulated $K_{0.4}Ce_{0.2}NbO_3$ by analogy with the TTB K_xWO_3. The three-dimensional $[NbO_3]_n$ network consists, as in ReO_3, cubic perovskite AMO_3, hexagonal tungsten bronze K_xWO_3, or again in pyrochlore structure, of NbO_6 octahedra sharing all their vertices with neighboring ones (Fig. 4a). The discussion concerning the niobium compound can be extended to the isostructural tantalum analogue.

The remarkable arrangement of this interconnected network of NbO_6 octahedra provides, within the structure and parallel to the [001] direction (the short cell parameter), three kinds of tunnels with pentagonal, square, and trigonal sections.

The precise determination of the structure allows us to specify that:

—K atoms are distributed in the pentagonal tunnels. Their crystallographic sites are fully occupied. Each potassium atom is surrounded by nine oxygens situated at the apices of a tricapped trigonal prism $O_{3ii}O_{3iii}O_5O_{3ix}O_{3x}O_{5vii'}$ $O_1O_{2xi}O_{2xiii}$; the mean value of K–O distances is 2.949 Å (2.943 Å for Ta species). Four oxygen O_4 which form with O_3 and O_5 the pentagonal section are more distant (Table 4). The coordination polyhedron around potassium definitely appears as a tricapped trigonal prism (CN9) (Fig. 4b).

—Ce atoms are inserted into the cuboctahedron, a typical perovskite-like site, filling up the square tunnels (Fig.

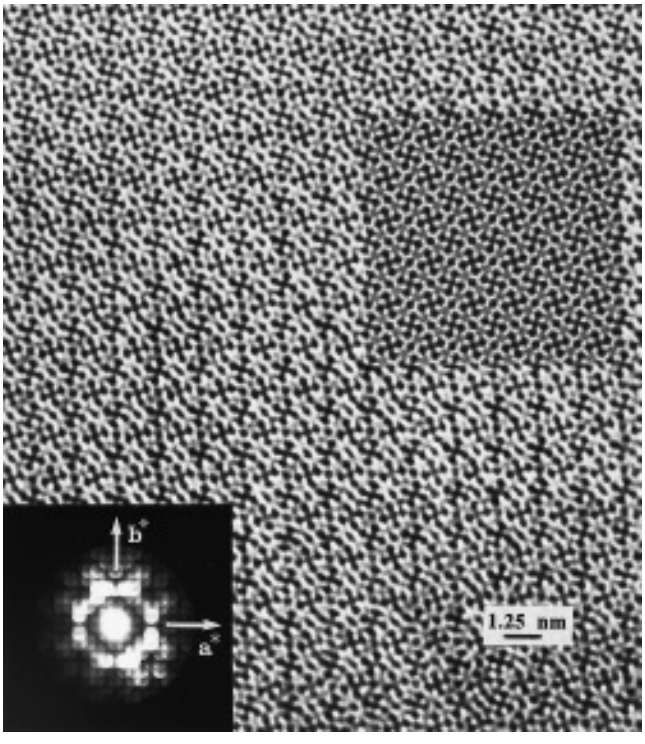

FIG. 5. High resolution electron microscopy of $K_4Ce_2Nb_{10}O_{30}$ obtained along the [001] zone axis and corresponding simulated image (defocalization −350 Å, thickness 25 Å).

4c). The 12-fold coordination of cerium III to oxygen exhibits normal Ce–O distances with an average value of 2.648 Å (2.638 Å for Ta species).

The formation of these stable phases with a network providing a nice cuboctahedral site for welcoming rare earth atoms could explain partly the facility with which CeO_2 looses oxygen, giving at last cerium in the +III oxidation state. Any ambiguity about the presence of Ce+III has been taken up by the magnetic measurements. However, it is always possible to envisage the existence of a few Ce atoms in the +IV oxidation state.

As for the TTB structure being formed with channels parallel to the **c** axis, the observations were performed along the [001] zone axis in order to obtain easily interpretable micrographs. Experimental HREM images obtained on a same area for two different defoci and their corresponding simulations are reported in Figs. 5 and 6. We have reported the TTB structure on which the Ce–Nb and K–Nb distances (Fig. 7a) or Nb–Nb distances (Fig. 7b) are drawn. The micrograph (Fig. 5) can then be easily interpreted: the cross-shape pattern corresponds to the atomic columns of cerium surrounded by the niobium ones. The dark spots isolated between the ''crosses'' also correspond to the niobium columns that delimit the pentagonal channels. Potassium atoms are situated in these channels. They are sketched as gray spots in Fig. 5. The experimental micrographs (Figs. 5 and 6) reveal a perfect periodicity of the structure without any defects. Particularly, all the pentagonal channels are filled with potassium. In Fig. 5, the gray contrast associated with the K atoms is lower than that due to the Ce and Nb columns; however, these contrasts can be very well simulated considering an occupancy factor of 1 for the potassium atoms. Furthermore, when changing the defoci the contrasts evolves to a more homogeneous one as is presented in Fig. 6 for −750 Å defocus. The atomic columns of Ce give fine white spot contrasts in a black square while the K and Nb columns present the same contrasts.

These two experimental micrographs obtained at different defoci are in good agreement with the simulated contrasts computed with the atomic positions deduced from the X-ray diffraction experiments. These HREM results show that all of the cerium and potassium sites are occupied and that TTB crystals are perfectly periodical without any defects at the atomic scale.

This study is a precise example of a perfect agreement between X-ray and HREM experiments and calculations. To our knowledge a complete single-crystal study of such phases has never been achieved. It is noted also that K, Nb, and Ce atoms can be recognized in a micrograph, the influence of their scattering power being clearly evident.

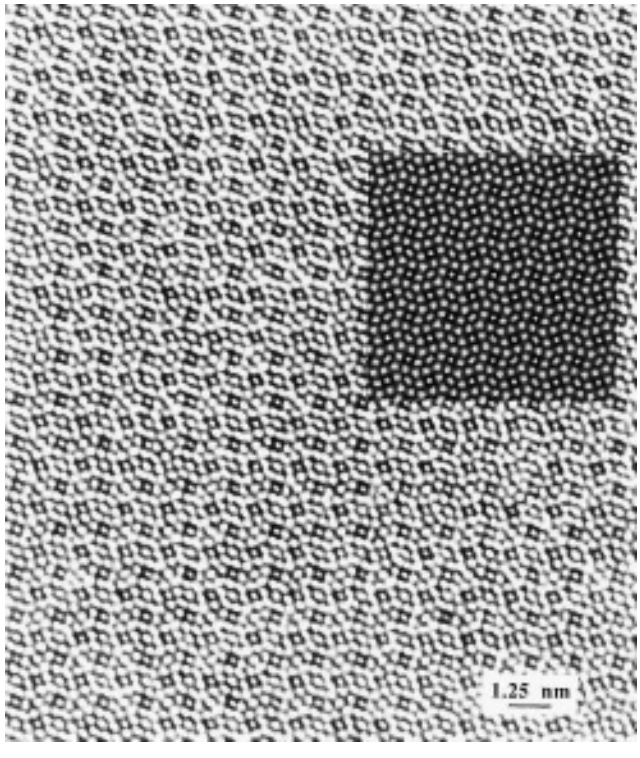

FIG. 6. High resolution electron microscopy of $K_4Ce_2Nb_{10}O_{30}$ obtained along the [001] zone axis and corresponding simulated image (defocalization −750 Å, thickness 25 Å).

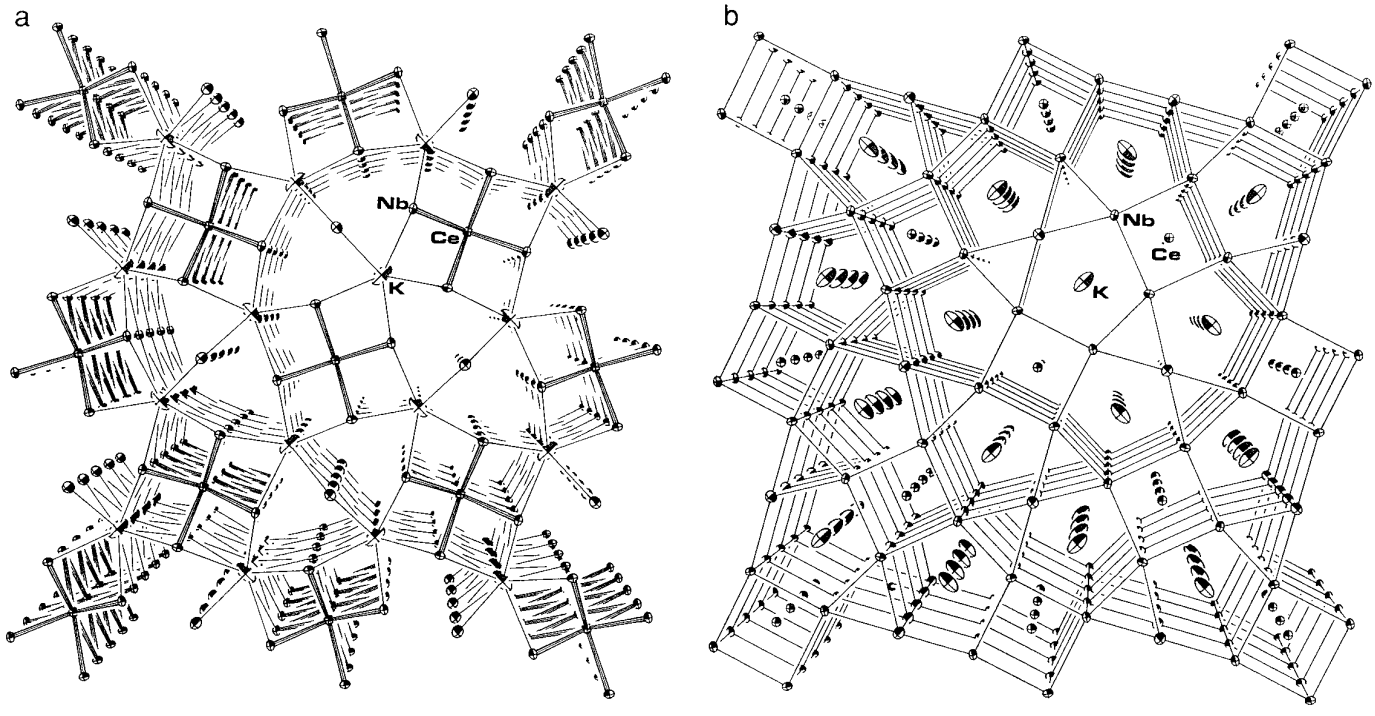

FIG. 7. Visualisation of the $K_4Ce_2Nb_{10}O_{30}$ structure: the interatomic Ce–Nb and K–Nd (a) or Nb–Nb (b) distances are represented.

From the chemistry point of view it is remarked that such phases, stabilizing Ce+III in the cuboctahedra of the structure, must be synthesized with CeO_2 as a starting material. Such a fact has already been noted in another synthesis, i.e., pyrochlores (21).

REFERENCES

1. A. Laurent, *Am. Chim. Phys. 2* **67,** 215 (1838).
2. A. Magnéli, *Arkiv. Kemi.* **1**(24), 213 (1949).
3. A. Magnéli, *Acta Chem. Scand.* **7,** 315 (1953).
4. P. B. Jamieson, S. C. Abrahams, and J. L. Bernstein, *J. Chem. Phys.* **48,** 5048 (1968).
5. B. A. Scott, E. A. Giess, G. Burns, and D. F. O'Kane, *Mater. Res. Bull.* **3,** 831 (1968).
6. J. Ravez, and J. P. Budin, *C.R. Acad. Sci.* **274,** 635 (1972).
7. L. Kihlborg, and A. Klug, *Chem. Scr.* **3,** 207 (1973).
8. J. P. Fayolle, F. Studer, G. Desgardin, and B. Raveau, *J. Solid State Chem.* **13,** 57 (1975).
9. A. Klug, *Mater. Res. Bull.* **12,** 837 (1977).
10. P. Sciau, Z. Lu, G. Calvarin, T. Roisnel, and J. Ravez, *Mater. Res. Bull.* **28,** 1233 (1993).
11. J. Pannetier, D. Franqui, and A. W. Sleight, *Mater. Res. Bull.* **28,** 989 (1993).
12. J. Galy, and B. Darriet, *Rev. Chim. Miner.* **11,** 513 (1974).
13. B. G. Hyde and S. Andersson (Eds.), "Inorganic Crystal Structures," Wiley–Interscience, New York, 1989.
14. F. Brik, R. Enjalbert, and J. Galy, *Mater. Res. Bull.* **29,** 15 (1994).
15. A. T. Casey, and S. Mitra, *in* "Theory and Applications of Molecular Paramagnetism" (E. A. Boudeaux and L. N. Mulay, Eds.), p. 271, Wiley–Interscience, New York, 1976.
16. A. C. T. North, D. C. Phillips, and F. S. Mathews, *Acta Crystallogr. Sect. A* **24,** 351 (1968).
17. D. T. Cromer, and D. Liberman, "International Tables for X-Ray Crystallography," Vol. IV, Kynoch Press, Birmingham, UK, 1974.
18. G. Sheldrick, "Program for Crystal Structure Determination," version SHELX-86, Oxford Univ. Press, Oxford, 1986.
19. C. K. Johnson, Ortep II report ORNL 5138, Oak Ridge National Laboratory, Oak Ridge, TN, 1976.
20. M. A. O'Keefe, and R. Kilaas, "HREM Analysis at the National Center for Electron Microscopy," XXIIth Western Regional Meeting for Electron Microscopy and Microbeam Analysis, Concord, CA, 1987.
21. F. Brik, Thesis, University of Toulouse, 1994.